metals

MDPI

Effects of Surface Severe Plastic Deformation on the Mechanical Behavior of 304 Stainless Steel

Yang Li [1,2], **Zhengtong Lu** [1], **Tingchao Li** [3], **Dalei Li** [1,2], **Jinsheng Lu** [2], **Peter. K. Liaw** [4] and **Yun Zou** [1,2,*]

1   School of Mechanical and Power Engineering, Zhengzhou University, Zhengzhou 450001, China; yangli@zzu.edu.cn (Y.L.); 15638217495@163.com (Z.L.); ldl@zzu.edu.cn (D.L.)
2   Henan Key Engineering Laboratory for Anti-fatigue Manufacturing Technology, Zhengzhou University, Zhengzhou 450001, China; lujinsheng2008@126.com
3   Technical Center of Dongfeng Motor Group Co., Ltd., Wuhan 430000, China; tingchao6688@163.com
4   Department of Materials Science and Engineering, The University of Tennessee, Knoxville, TN 37996, USA; pliaw@utk.edu
*   Correspondence: yunzou@zzu.edu.cn; Tel.: +86-371-67781231

check for updates

Abstract: In this study, two innovative surface severe plastic deformation (SSPD) methods, namely abrasive waterjet peening (AWJP) and ultrasonic nanocrystal surface modification (UNSM), were applied to a 304 stainless steel to improve the mechanical behavior. The surface roughness, microstructure, residual stress, hardness, and tensile mechanical properties of the alloy after the two SSPD treatments were studied systematically. The results show that both the AWJP and UNSM treatments have greatly positive effects on the mechanical-properties improvements by successfully introducing a hardening layer. Especially the UNSM-processed specimen possesses the most outstanding comprehensive mechanical properties (high strength with the comparable ductility). The yield strength with the UNSM treatment is 443 MPa, corresponding to the 109% and 19% improvements, as compared to that of the base (212 MPa) and AWJP-treated specimens (372 MPa). The results can be attributed to a much thicker hardening layer (about 500 μm) and a better surface integrity with lower roughness (Ra: 0.10 μm) formed by the UNSM technique.

1. Introduction

Metal engineering materials often fail as a result of the overload, corrosion, high speed, fatigue, and wear, causing catastrophic consequences. Lu et al. (1999) [1] introduced surface Nanocrystallization (SNC) of metallic materials and pointed out that the failure of metal materials (fatigue fracture, fretting fatigue, wear, and corrosion, etc.) is very sensitive to the surface properties. Bregliozz et al. (2004) [2] studied the friction and wear properties of AISI 304 austenitic stainless steel with different grain sizes. The results show that fine-grain steels are more wear resistant and exhibit lower coefficient of friction compared to coarse-grain steels for all the load range and relative humidities analyzed. Järvenpää et al. (2020) [3] reported the reversion of deformation induced martensite to fine-grained austenite to increase yield strength of metastable austenitic stainless steels without impairing much their ductility. Di Schino et al. (2002) [4] investigated the effects of both the substrate microstructure and coating composition on the tribological properties of a high-nitrogen austenitic stainless steel. Founded that with the refinement of the matrix structure, the duration of low friction performance was improved. Therefore, surface-strengthening technology is necessary in order to improve the surface properties of

the materials. Using surface severe plastic deformation (SSPD) method can change the surface quality and mechanical properties. In recent years, many SSPD techniques have been previously explored to improve the properties of bulk materials. Aviles et al. (2019) [5] applied shot peening (SP) to the DIN 34CrNiMo6 alloy steel, after shot peening, the surface roughness *Ra* = 1.41 μm, and the maximum residual stress is about 600 MPa, and the fatigue limit of the specimens increased by 39%. Tian et al. (2007) [6] investigated the fatigue behaviors of a Ni-based C-2000 superalloy subjected to the surface nanocrystallization and hardening (SNH) process, the results show that the nanostructured surface layer, work-hardened region, and residual compressive stress introduced by SNH could enhance the fatigue strength. Tao et al. (2002) [7] proposed a grain-refinement mechanism induced by plastic deformation during the surface-mechanical-attrition treatment (SMAT) in Fe. After SMAT the grain refinement layer reaches a depth of 110 μm, of which nanostructured layer is 15 μm. Kim et al. (2019) [8] studied microstructural evolution and mechanical properties of the ultrasonic nanocrystalline surface modification (UNSM) processed twinning-induced plasticity (TWIP) steels were investigated. After the UNSM treatment, the yield strength of the material increased from 550MPa to 800 MPa, and the tensile strength increased from 1000 MPa to 1200 MPa. Proved that UNSM can effectively improve the mechanical properties of materials. The fundamental principle of SSPD is to produce the partial plastic deformation near the surface by impact or extrusion, form a certain depth of the deformation layer accompanying with the residual compressive stress and microstructural change, and thus improve the material properties.

Among them, the waterjet peening (WJP) technology is a metal-strengthening technology based on the deformation-strengthening mechanism. In the 1980s, Zafred (1987) [9] first proposed the use of high pressure water shot peening to strengthen the metal surface. The principle of WJP is to use water as a working medium, and the high-energy water jet impacts the surface of the metal parts at high speeds, which makes the surface material of the parts produce the plastic deformation below the recrystallization temperature, and form a certain depth of a hardening layer. Azhari et al. (2012) [10] improved the mechanical properties of an austenitic stainless steel using the WJP process. By using surface integrity to evaluate the performance of different parameters in the WJP process. increase in the number of jet passes as well as pressure leads to a higher roughness and more erosion of the surface, it also increases subsurface hardness and hardened layer depth. The feed rate shows a reverse effect on the surface roughness and erosion. Compared to WJP, the introduction of abrasives in abrasive water jet (AWJP) can introduce greater deformation and residual compressive stress [11]. Arola et al. (2006) [12] used AWJP to process AISI 304. It was found that AWJP results in compressive residual stress and is primarily influenced by the abrasive size and treatment pressure. After treatment, the maximum residual stress of AISI 304 is −460 MPa. UNSM is also one of the surface-deformation-strengthening methods. For the equipment, the UNSM mainly contains an ultrasonic generator, ultrasound transducer, ultrasonic horn, and impact head. The ultrasonic generator and transducer convert the high-frequency alternating electric energy into the mechanical vibration. The typical ultrasonic transducer has a vibration frequency of 15–30 kHz, and its output amplitude is small, generally less than 10 μm. The amplitude lever is connected to the transducer and amplifies its vibration amplitude. Impacted by the ultrasonic horn, the impact head strikes the workpiece surface at a high frequency. The extreme stress impact of thousands of times per second makes the surface of the workpiece more plastic deformation than the traditional surface treatment. At present, UNSM has been applied to many materials. Wu et al. (2013) [13] treated S45C nitrided steel with UNSM. Compared with the un-UNSMed samples, the enhancement of the surface hardness, and the fatigue strength were obtained after UNSM-treatment, meanwhile the nitrogen diffusion rate near the surface layer is improved. Hou et al. (2017) [14] utilized UNSM technique to induce plastic strain on metal surfaces, was applied to an AZ31B magnesium alloy. Significant improvement in hardness, yield stress and wear resistance was achieved after the UNSM-treatment. Meanwhile, the corrosion behavior of UNSM-treated AZ31B was not compromised compared with the untreated samples. Propose the possibility of applying UNSM technology to process magnesium alloys in the field of biomedicine in addition, Amanov et al. (2017) [15] reported that the development

of combined heat treatment and UNSM technique was successfully demonstrated the feasibility of an increase in hardness and wear resistance of Ti-6Al-4V alloy. Zhang et al. (2017a) [16] found that the UNSM-treatment can significantly improve surface finish, decrease subsurface porosity, increase surface hardness, and at the same time change the residual stresses from tensile to compressive. Through the rotation bending fatigue test, it is found that UNSM-treatment can significantly improve the fatigue performance of the component. These research results indicated that UNSM could significantly improve the mechanical properties of the material.

The 304 stainless steel is widely used in various fields because of its good corrosion resistance, heat resistance, and hot workability. Many different SSPD treatment methods were applied to the 304 stainless steel to improve the mechanical properties. Yasuoka et al. (2013) [17] utilized UNSM technique to improve the fatigue strength of SUS304 austenite stainless steel, after UNSM-treatment gradient nanocrystalline plastic deformation layer with increased hardness was created at the specimen surface. The plastic deformation layer was 30 to 200 μm, and the top grain is refined to the nanometer level. And the fatigue strength was improved by approximately 80%, the hardened surface layer was assumed to be the main reason for the improvement in the fatigue strength. Zhang et al. (2003) [18] fabricated a nanostructured surface layer on an AISI 304 stainless steel with low stacking-fault energy by means of the SMAT. Ye et al. (2014) [19] Studies the microstructural evolution and mechanical properties of 304 stainless steel treated by UNSM. After UNSM-treatment, martensite is formed, and a large amount of surface compressive residual stress (−1400 MPa) and hardening are generated. The work-hardened surface layers (3.5 times the original hardness) and high magnitude of compressive residual stresses lead to significant improvement in fatigue performance, the experimental results show that the fatigue limit has increased by 100 MPa. There were the very high compressive stress and deep residual stress layer in the surface layer. As a result, the UNSM significantly improved the fatigue strength of the 304 stainless steel.

In the present research, two innovative SSPD methods, AWJP and UNSM, were utilized to process the 304 stainless steel. The surface morphology, microstructure, residual stress, hardness, and tensile mechanical properties of AWJP/UNSM-treated 304 materials were systematically studied. The aim is to find a valid method to improve the surface quality and mechanical properties and illuminate which factor has the greatest contribution to the improvement of mechanical performance and bedding for the subsequent work.

2. Experimental Details

2.1. Sample Preparations

The rolled 304 stainless-steel plate with the measured chemical composition of 0.068 C, 0.58 Si, 0.71 Mn, 0.024 P, 0.004 S, 18.20 Cr, 8.45 Ni, and balance Fe (in weight percent, wt. %) was used. Samples ($100 \times 100 \times 2.0$ mm) were cut by electric discharge machining from the rolled plate, and then solution-treated at 1363 K for 60 min, followed by water quenching. All samples were abraded with SiC grinding papers to 1000# before further treatments and tests.

In order to improve the mechanical properties of the materials and make the comparison, two SSDP methods (AWJP and UNSM) were applied to the 304 stainless steel plate in this study. Schematic diagrams of the AWJP and UNSM processes are illustrated in Figure 1. The AWJP experiments were carried out on the GlobalMAX1530 waterjet machine of OMAX Corporation (Kent, WA, USA), and the medium used were the glass pellets with a diameter of 0.5 mm to obtain lower surface roughness. In the AWJP experiments, as illustrated in Figure 1a, the water pressure is 50 MPa, and the nozzle geometry used in this experiment is a round one with a diameter of 1.0 mm, and the incidence angle was set at 90° (the nozzle was perpendicular to the specimen surface.). The nozzle moving speed is 400 mm/min, the target distance is 15 mm, and the interval between each pass is 0.25 mm. The UNSM experiments were carried out by HC30C UNSM system of Shandong Huayun Electromechanical Technology (Jinan, China). In the UNSM process, as illustrated in Figure 1b, a tungsten-carbide ball

with a diameter of 14 mm attached to an ultrasonic device scans over the material surface while striking it at a high frequency of 28 kHz, which is greater than the often used frequency of 20 kHz. Ma et al. (2017) [20] utilized a tungsten carbide tip to streike the sample surface at 20 kHz frequency, and the compressive residual stresses with a maximum magnitude of 1130 MPa were induced in the near-surface region after UNSM treatment. Kheradmandfard et al. (2017) [21] produced a gradient nanostructured layer by UNSM treatment, a ball-shaped tungsten carbide tip striking the surface of β-type titanium alloy with the frequency of 20 kHz. In this study, a static load of 0.3 MPa is applied to the ball against the material surface. The scanning speed is 3500 mm/min., and the interval is 0.1 mm. Hereafter, the base specimens are labeled as BASE while the AWJP-treated ones and UNSM-treated ones are labeled as AWJP and UNSM, respectively.
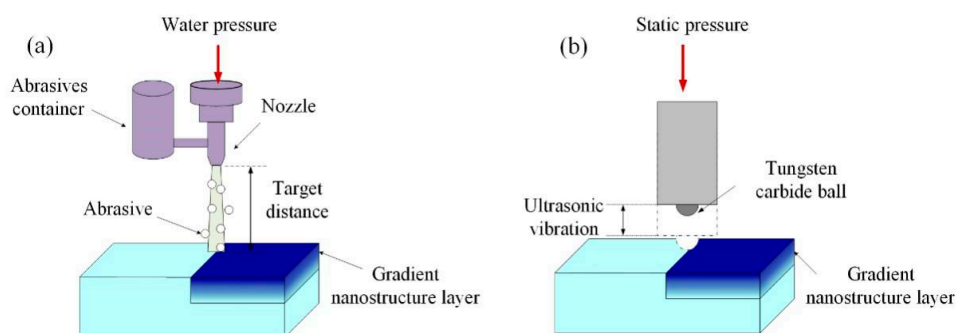
Figure 1. Schematic diagrams of the (**a**) AWJP and (**b**) UNSM processes.

2.2. Material Characterization

To reveal the subsurface microstructure, the samples were cut along the cross-section, metallographically ground and polished, followed by etching in the aqua regia. The microstructure was analyzed, using the optical microscopy (OM) (Keyence, Osaka, Japan) and scanning electron microscopy (SEM, Zeiss Auriga Compact, Jena, German). The three-dimensional (3D) surface topography and surface roughness (*Ra*) of the materials were characterized, using a Bruker's NPFLEX™ 3D Surface Metrology System (Bruker, Karlsruhe, German). A measurement area of about 1502×1502 μm^2 was covered. Light and dark colors indicated peak and valley regions, respectively. The surface roughness (*Ra*) is an average of at least five roughness values.

The residual stresses of the material surface before and after AWJP/UNSM treatments were measured by the X-ray stress analyzer (LXRD, Proto, ON, Canada) with a Ni filter (the Cr-K$_\alpha$ radiation for the martensite and Mn-K$_\alpha$ radiation for the austenite). The current and voltage were 25 mA and 30 kV, respectively. The XRD system was calibrated by a stress-free sample. The shifts of the α martensite phase peak, {211}$_\alpha$, with the 2θ value of 156.4° and γ austenite phase peak, {311}$_\gamma$, with a 2θ value of 152.8° were detected in the measurements. An average of at least five sets of residual compressive stresses data was recorded.

The X-ray diffraction (XRD) analysis of the material surface before and after AWJP/UNSM treatments were measured by the PANalytical Empyrean XRD equipment the working voltage 45 kV, working current 40 mA, Cu-Kα radiation, scanning angle range 30–110°, scanning speed 6°/min. Based on Jade 6.0 software (Materials Data, Livermore, CA, USA), the phase composition of 304 stainless steel was analyzed according to the XRD pattern measured by the test.

The distribution of the micro Vickers hardness value along the AWJP/UNSM treated surface to the base of the specimens was conducted, using the HV-1000 Vickers hardness tester (Beijing Times Mountain Peak Technology, Beijing, China) with an experimental force of 100 g employing a diamond pyramid indenter, and the loading time of 15 s. An average hardness value of five points at every depth was selected for description.

Tension tests were carried out at a strain rate of 1×10^{-3} s^{-1} on an MTS tensile tester (MTS 370.02) (MTS Systems Corporation, Eden Prairie, MN, USA) at room temperature. An extensometer

was applied during tension tests. According to the GB/T228.1-2010, tensile specimens are produced. The dimensions of the specimens are shown in Figure 2. Both of two opposite faces of the gauge area were processed by AWJP/UNSM treatments before the tensile test.
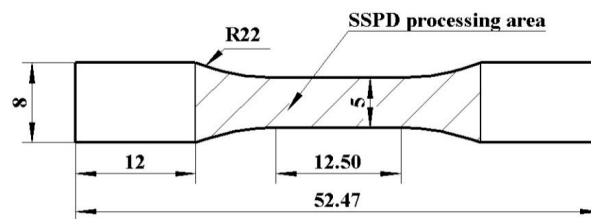

Figure 2. Sketch of tensile specimen (unit: mm).

3. Results

3.1. Surface Morphology, Microstructures, and Retained Austenite Content

3.1.1. Surface Morphology

Surface roughness is closely related to the material strength, wear resistance, corrosion resistance, and sealing performance of mechanical components. The surface of the rough part contains a large number of grooves, which will cause stress concentration, and fatigue fracture cracks of the material often originate in these stress concentration parts [22], it will reduce the mechanical properties of the material The rougher the surface, the smaller the effective contact area. Then the greater the pressure, the higher the friction resistance, and the faster the wear. Compared with smooth surfaces, rough surfaces have a larger contact area with corrosive gases and liquids and are more prone to corrosion. Rough surfaces do not fit tightly, and gases or liquids leak through gaps between contact surfaces. Therefore, the roughness of materials will directly affect the performance and life of machinery. Usually, the SSPD-strengthening treatments (e.g., shot-peening treatments) often increase the surface roughness of the workpiece, resulting in the microscopic-stress concentration. It will partially offset the beneficial effect of the compressive residual stress and have a negative effect on the mechanical performance of the parts. The 3D surface topographies and the average roughness, *Ra*, are shown in Figure 3. The matrix roughness, *Ra*, is 0.29 μm. Applying AWJP to 304 stainless steel, the roughness, *Ra*, of the AWJP sample is 1.912 μm. While the surface roughness reached 0.10 μm after UNSM treatment. That is, the AWJP processes increase the surface roughness (increased by about 624%), while the UNSM technology can greatly reduce the roughness (reduced by about 66%), relative to the untreated sample.
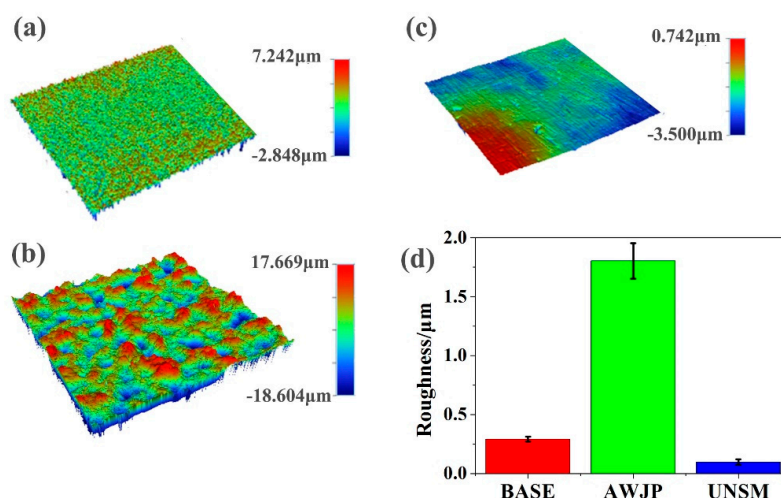

Figure 3. The 3D surface topographies of (**a**) BASE, (**b**) AWJP, and (**c**) UNSM specimens, and (**d**) responding surface roughness, Ra, of the specimens.

3.1.2. Microstructures

The cross-sectional microstructures of the BASE, AWJP, and UNSM specimens are, respectively, shown in Figure 4a–c. The microstructure of the untreated sample (Figure 4a) is typically austenitic. It can be seen from Figure 4b,c that the sample shows a gradient microstructure with a SPD layer, and the near-surface grain is deformed to some extent but not obvious after AWJP/UNSM treatments. The deformation layer depth of the AWJP specimen is about 80 μm. The deformation layer depth of the UNSM specimen is 200 μm (Figure 4c), which is obviously thicker than that of the AWJP one (Figure 4b). Besides, both of AWJP and UNSM treatments specimen contains a large number of deformation twins, this trend explains that the deformation mode is mainly the deformation twins, Zhang et al. (2003) [18] reported that twins are the universal deformation mechanism of the 304 stainless steel during the grain refinement, which is consistent with our research. The degree of plastic deformation gradually decreases with the increase of the distance to the surface, which can be ascribed to the decreased plastic strain in the depth direction.
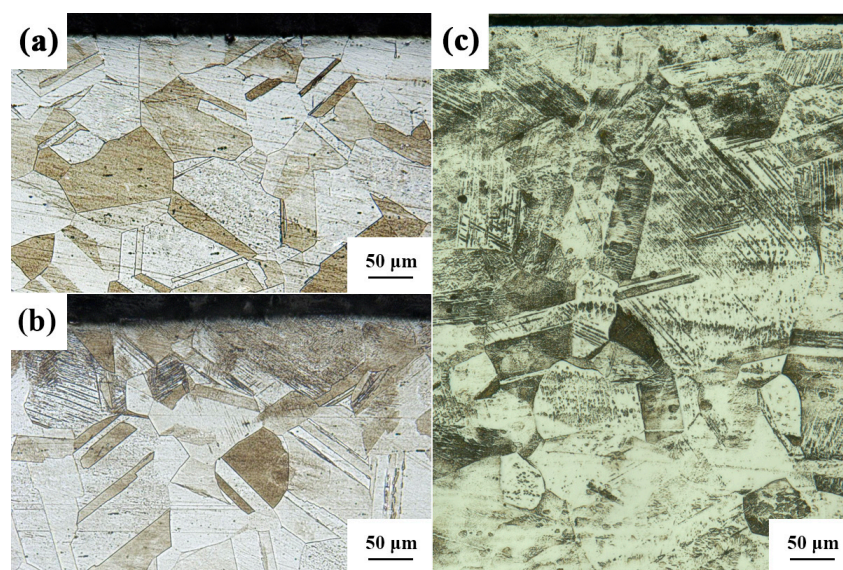
Figure 4. The cross-sectional microstructures of (**a**) BASE, (**b**) AWJP, and (**c**) UNSM specimens.

Figure 5 is the SEM images on the top surface of AWJP and UNSM specimens. It can be seen that there are many erosions and pits on the AWJP-treated surface left by the impact of the glass pellets and hydrodynamic erosion (Figure 5a). Some stripes can be seen on the surface of UNSM-treated specimen, which can be ascribed to the traces of UNSM ball movement. Compared with the AWJP-treated surface, the surface of UNSM-treated specimen is much smoother and the surface grains are obviously refined (Figure 5b).
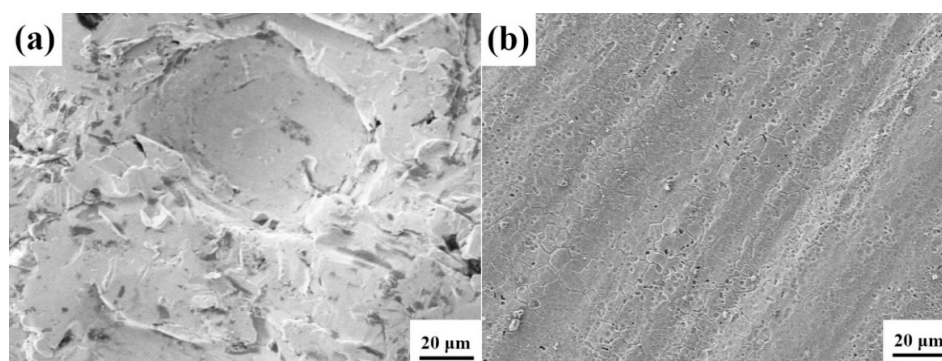
Figure 5. The SEM images at the top surface of (**a**) AWJP and (**b**) UNSM specimens.

3.1.3. X-ray Diffraction

Figure 6 is the X-ray diffraction pattern of BASE, AWJP, and UNSM specimens. Compared with the BASE sample, the X-ray diffraction peak of martensite was found in the specimens after AWJP and UNSM treatments, indicating that martensite phase transformation was induced. The intensity of the diffraction peak of austenite decreases significantly, and the peak width slightly widens after AWJP and UNSM treatments, which may be due to the generation of internal stresses [15]. The occurrence of high strain, severe plastic deformation, and grain refinement on the surface of the material are responsible for the lower intensity of the diffraction peak and the broadening of the peak [23]. So, it can be judged that both of AWJP and UNSM treatments caused severe plastic deformation, grain refinement, and martensite phase transition on the surface of 304 stainless steel.
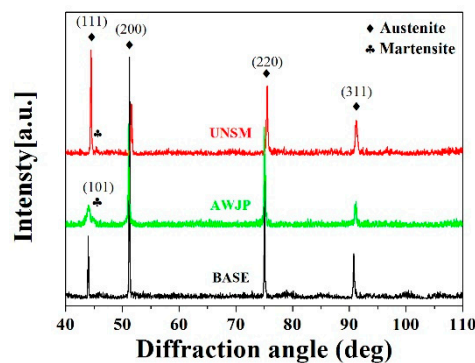
Figure 6. The X-ray diffraction pattern of BASE, AWJP, and UNSM specimens.

3.2. Mechanical Properties
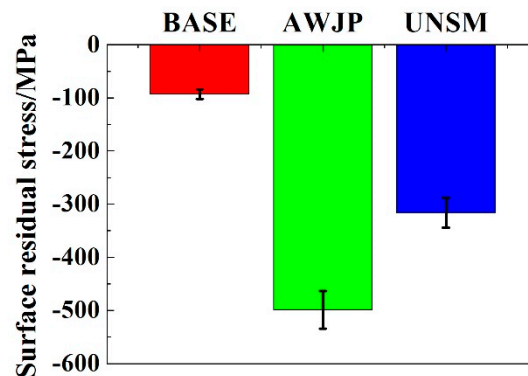
3.2.1. Residual Stress

Fu et al. (2013) [24] reported that the surface residual stress is of interest because it may affect the material-mechanical performance. Muhammet et al. (2019) [25] proposed that the residual stresses near the top surface layer were evaluated by the X-ray diffraction (XRD) $\sin^2\Psi$ method. The test principle is based on the fact that the produced residual stress in crystalline materials can result in an interplanar spacing change, and thus be accessed indirectly by measuring the d-spacing. The $\sin^2\Psi$ technique is the most popular method used for measuring the residual stress by the XRD method, where the diffraction peak is determined at the high range of 2θ angles. Then, the XRD system is adjusted in this angle, and d-spacing of crystal planes is measured in different positions. The residual stresses were calculated after mathematical simplifications as follows:

$$\sigma = \frac{E}{(1+\nu)\sin^2\Psi}\left[\frac{d_\Psi - d_0}{d_0}\right] \qquad (1)$$

where σ is the residual stress, E is Young's modulus, ν is the Poisson's ratio, d_0 is the d spacing of stress-free crystal planes, and d_Ψ is the d spacing of stressed crystal planes in the Ψ direction.

Due to the fact that the martensite-phase transformation can be induced by the severe plastic deformation, the residual stresses in both of the two phases, austenite and martensite, were evaluated. However, the α martensite phase peak, $\{211\}_\alpha$, is very weak, and the detected residual stresses value is not available. Thus, residual stresses at the top surface exhibited here were just measured by the γ-austenite phase peak, $\{311\}_\gamma$, along the traveling direction of the AWJP/UNSM tip. The measured surface residual stresses of the BASE, AWJP, and UNSM specimens are illustrated in Figure 7. The average surface residual stress value of the BASE sample, AWJP, and UNSM samples were about −93, −499, and −316 MPa, respectively. This indicates that both of the AWJP and UNSM

treatments can induce higher residual compressive stresses, which is beneficial to the improvement of mechanical properties.

Figure 7. Surface residual stress of the 304 stainless steel BASE, AWJP, and UNSM specimens.

3.2.2. Hardness

The micro Vickers hardness depth profiles of 304 stainless-steel specimens before and after AWJP/UNSM treatments are compared in Figure 8. The hardness values were measured from the treated top surface to the cross-sections of the specimens at different depths. An average of 5 points measurements at the same depth beneath the surface, and especially, the top-surface hardness results were obtained by testing the processed surface. At the top surfaces of the AWJP-treated and UNSM-treated specimens, the AWJP-treated specimen has higher hardness, which is as high as 387 HV, corresponding to the 98% improvement, as compared to the BASE alloy (195 HV); and the average hardness of the top surface UNSM-treated specimens are 288 HV, corresponding to the 48% improvement, as compared to the BASE alloy. It can be clearly seen that the hardening effect is gradually weakened as being deeper into the layer due to the gradient nature of the plastic strain in the depth direction. The hardening layer of the AWJP-treated specimen may extend up to a depth of about 300 μm, lower than that of the UNSM-treated specimen with a 500 μm depth, implying a more significant hardening effect with the UNSM technology.
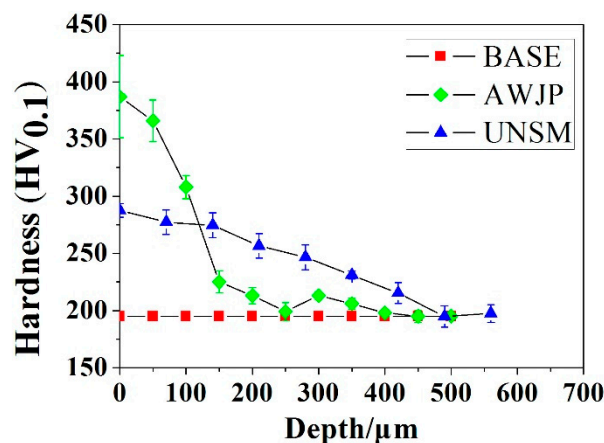

Figure 8. Hardness-depth profile of the 304 stainless-steel BASE, AWJP, and UNSM specimens.

3.2.3. Tensile Properties

The engineering stress-strain curves of the 304 samples before and after AWJP/UNSM treatments tested at the ambient temperature are demonstrated in Figure 9. The tensile yield strength at the 0.2% offset ($\sigma_{0.2}$) has increased from 212 to 372 and 443 MPa after AWJP and UNSM treatments, corresponding to the 75% and 109% improvements, respectively. The yield strength of AWJP and

UNSM-treated samples are also much higher than that of the pure waterjet peening (no abrasive) treated samples (~255 MPa) in our previous study [26]. The ultimate tensile strength of the material after UNSM treatments tested is 817 MPa, which is 24% higher than that of the BASE (654 MPa). The ultimate tensile strength of AWJP-treated specimen did not increase significantly. Elongations to fracture of the BASE, AWJP, and UNSM samples are 74%, 75%, and 69%, implying that all the samples have reasonably good tensile ductility.
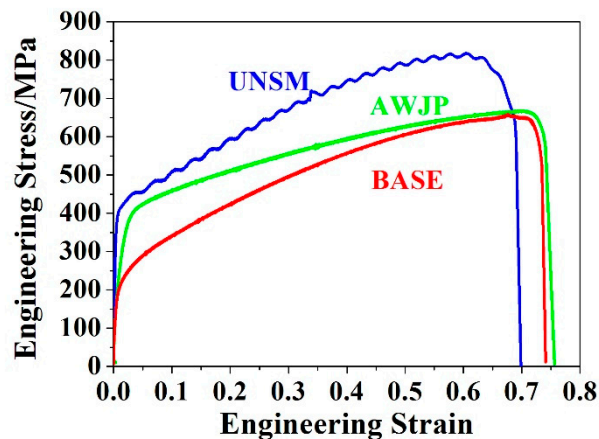
Figure 9. The engineering stress-strain curves of the 304 stainless-steel BASE, AWJP, and UNSM specimens.

Figure 10 is the fracture morphologies of the UNSM-treated specimen, and corresponds to the b (interior) and c (near-surface) positions marked in Figure 10a, respectively. Figure 10b shows that fine dimples are evenly distributed in the interior one, staying in the original ductile fracture. Figure 10c shows shallow and elongated dimples in the near-surface zone, indicating poor ductility in the severely deformed region. The closer to the surface, the shallower the dimples, this shows that the closer to the surface, the worse of the plasticity of the material. The poor ductility in the near-surface zone may cause by the formed martensite phase and severely deformed layer.
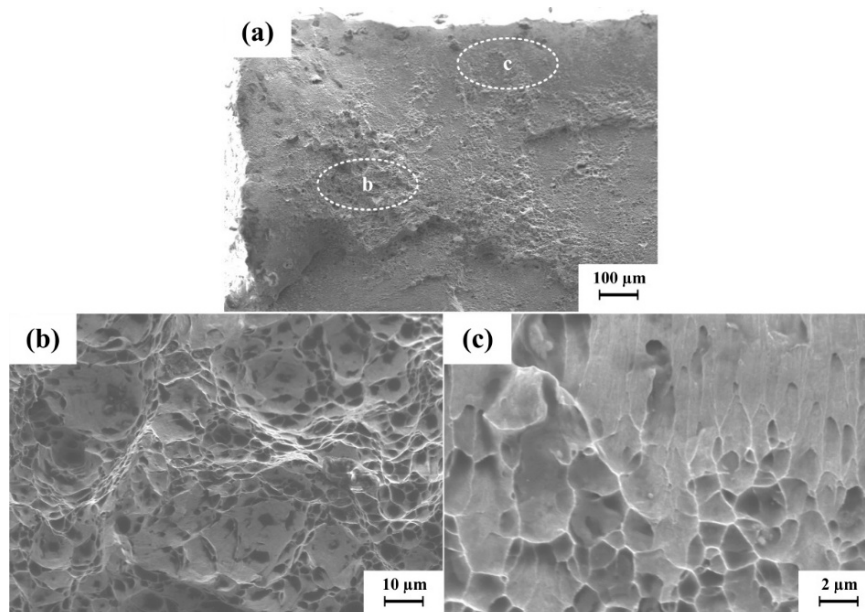
Figure 10. The fracture morphology of the 304 stainless-steel UNSM specimen.

4. Discussion

Surface roughness is closely related to the material strength, wear resistance, corrosion resistance, and sealing performance of mechanical components. Comparing the roughness of the samples treated with UNSM and AWJP, it could be found that UNSM can obviously improve the surface roughness of the 304 stainless steel, while AWJP is not beneficial for improving the surface roughness. During the UNSM process, large and uniform plastic deformation occurs on the surface of the specimen because of the UNSM-tip striking, which is similar to the ball-burnishing process. The large and uniform plastic flow causes the roughness flows from the peaks to the valleys, leading to much better surface finishing and giving better mechanical performances. In contrast to the flat and unobvious flaws on the surface of the UNSM sample, there are many erosions and pits on the surface of the AWJP-treated sample, and these erosions and pits may be detrimental for the mechanical properties.

It is well known that the formation of surface residual stress is related to the SSPD. In the process of AWJP, the surface residual stress is induced by the repetitive severe plastic deformation of a thin surface zone caused by the bombardment of high-frequent water drops and a with great velocities on the material surface. During the UNSM process, the continuous impact of the tungsten carbide ball accompanied by the high-energy ultrasonic vibration on the material surface will also lead to the repetitive local severe plastic deformation. Because of the unequal plastic deformation between the surface and the internal layer of the material, the SSPD treatment, AWJP, and UNSM induce a surface residual stress at the surface and a compensation tensile residual stress inside the specimen away from the surface. As we know, material failure often initiates on the surface and expands due to the tensile stress. The surface residual stress induced by AWJP and UNSM treatments can effectively suppress the crack initiation and impede its propagation by counteracting the tensile stress, thereby improving the mechanical properties.

In general, the strength and ductility of materials are inversely related, that is, materials with the high strength typically have the low ductility. Whereas, the 304 stainless steel treated with AWJP and UNSM processes in this study has the higher tensile yield strength with preserving the great ductility. Especially, the UNSM one has the most outstanding comprehensive mechanical properties, which can be attributed to the powerful drive of ultrasonic vibrations imposed with the static load instead of the single high-frequent impact of water drops and glass pellets impact during AWJP processing. The repeated ultrasonic vibrations imposed with static loads makes the metal surface produce greater plastic strains, more deeper hardening effects, and smoother surfaces than those introduced by the single high-frequent impact of water drops and glass pellets with the high kinetic energy, which causes obvious erosions and voids, detrimental for the mechanical improvement based on our study. Besides, it is noteworthy that a peculiar phenomenon, the serrations (a wavy pattern like a saw tooth), is observed in the engineering stress-strain curve of the UNSM-treated sample, resulting from the inhomogeneous plastic flow of the gradient microstructure of the deeper hardening layer by the powerful UNSM treatment during tensile deformation. Zhang et al. (2017b) [27] reported that the deformation mechanism in alloys is known as the Portevin-Le-Chatelier (PLC) effect, it is derived from dynamic strain aging (DSA). In DSA, the interaction between dislocations and solute atoms in the gradient microstructure results in repeated pinning of dislocations, and thus, leads to the enhanced work hardening, which contributes to outstanding comprehensive mechanical properties.

UNSM causes severe plastic deformation on the near-surface layer of the material. The plastic strain and strain rate are gradually decreasing from the surface to the interior, which is also verified by the microstructure (Figure 4c). Wang and Ma (2004) [28] reported that nanocrystalline and ultrfine-grained metals to become unstable during tensile deformation is related to the diminishing strain hardening capacity and the inadequate strain rate hardening by Considère criterion. In addition, Ye et al. (2014) [19] reported that ductility of the material is essentially determined by its strain hardening capacity, which is the capacity to accumulate dislocations generated during plastic deformation.

According to the Considère criterion, the uniform elongation holds in a tensile test until the onset of the localized deformation, which is governed by

$$\left(\frac{\partial\sigma}{\partial\varepsilon}\right)_{\dot{\varepsilon}} = \sigma \tag{2}$$

where σ is the true stress, ε is the true strain, and $\dot{\varepsilon}$ is the strain rate. This equation indicates that the material ductility is substantially determined by its strain-hardening capacity, which is the ability to accumulate dislocations generated during plastic deformation. The coarse-grained inner regions have more capacities of the dislocation accumulation and show the ductile fracture during tensile tests. On the contrary, the fine-grained upper regions have a limited ability to further accumulate dislocations and show brittle fracture during stretching. Consequently, the special gradient microstructure formed by the UNSM treatment can suppress the strain localization and allow the materials to maintain high strength and toughness.

5. Conclusions

In this study, two innovative SSPD methods, namely AWJP and UNSM, were applied to 304 stainless steel. The surface morphology, microstructure, residual stress, hardness, and tensile mechanical properties of AWJP/UNSM-treated 304 materials were systematically studied. The results have shown that a noticeable hardening layer and high levels of surface compressive residual stresses were successfully introduced by the two SSPD methods, which thus contribute to both the high hardness and strength. The UNSM-processed specimen possessed the most outstanding comprehensive mechanical properties (high strength with the comparable ductility). The yield strength reaches 443 MPa, corresponding to 109% and 19% improvements, as compared with that of the BASE (212 MPa) and AWJP treated specimens (372 MPa) respectively, while the ultimate tensile strength reaches 817 MPa corresponding to 24% and 22% improvements, as compared with that of the BASE (654 MPa) and AWJP treated specimens (667 MPa) respectively. This trend can be attributed to the formed much thicker hardening layer (about 500 μm) and better surface integrity with the lower roughness (*Ra*: 0.10 μm) under the more powerful drive of ultrasonic vibrations imposed with a static load using the UNSM technique.

References

1. Lu, K.; Lu, J. Surface Nanocrystallization (SNC) of Metallic Materials-Presentation of the Concept behind a New Approach. *J. Mater. Sci. Technol.* **1999**, *15*, 193–197.
2. Bregliozzi, G.; Ahmed, S.I.-U.; Di Schino, A.; Kenny, J.M.; Haefke, H. Friction and wear behavior ofaustenitic stainless steel: Influence of atmospheric humidity, load range, and grain size. *Tribol. Lett.* **2004**, *17*, 697–704. [CrossRef]
3. Järvenpää, A.; Jaskari, M.; Kisko, A.; Karjalainen, P. Process and properties of reversion-treated austenitic stainless steels. *Metals* **2020**, *10*, 281. [CrossRef]

4.　Di Schino, A.; Valentini, L.; Kenny, J.M.; Gerbig, Y.; Ahmed, I.; Hefke, H. Wear resistance of high-nitrogen austenitic stainless steel coated with nitrogenated amorphous carbon films. *Surf. Coat. Technol.* **2002**, *161*, 224–231. [CrossRef]

5.　Aviles, A.; Aviles, R.; Albizuri, J.; Pallares-Santasmartas, L.; Rodriguez, A. Effect of shot-peening and low-plasticity burnishing on the high-cycle fatigue strength of DIN 34CrNiMo6 alloy steel. *Int. J. Fatigue* **2019**, *119*, 338–354. [CrossRef]

6.　Tian, J.W.; Villegas, J.C.; Yuan, W.; Fielden, D.; Shaw, L.; Liaw, P.K.; Klarstrom, D.L. A study of the effect of nanostructured surface layers on the fatigue behaviors of a C-2000 superalloy. *Mat. Sci. Eng. A* **2007**, *468*, 164–170. [CrossRef]

7.　Tao, N.R.; Wang, Z.B.; Tong, W.P.; Sui, M.L.; Lu, J.; Lu, K. An investigation of surface nanocrystal-lization mechanism in Fe induced by surface mechanical attrition treatment. *Acta. Mater.* **2002**, *50*, 4603–4616. [CrossRef]

8.　Kim, J.G.; Moon, J.H.; Amanov, A.; Kim, H.S. Strength and ductility enhancement in the gradient structured twinning induced plasticity steel by ultrasonic nanocrystalline surface modification. *Mater. Sci. Eng. A* **2019**, *739*, 105–108. [CrossRef]

9.　Zafred, P.R. High pressure water shot peening. *Ausz Eur Patentanmeld I* **1987**, *15*, 719.

10.　Azhari, A.; Schindler, C.; Kerscher, E.; Grad, P. Improving surface hardness of austenitic stainless steel using waterjet peening process. *Int. J. Adv. Manuf. Technol.* **2012**, *63*, 1035–1046. [CrossRef]

11.　Sadasivam, B.; Hizal, A.; Arola, D. Abrasive waterjet peening with elastic prestress: A parametric evaluation. *Int. J. Mach. Tools Manuf.* **2009**, *49*, 134–141. [CrossRef]

12.　Arola, D.; Alade, A.E.; Weber, W. Improving fatigue strength of metals using abrasive waterjet peening. *Mach. Sci. Technol.* **2006**, *10*, 197–218. [CrossRef]

13.　Wu, B.; Wang, P.P.; Pyoun, Y.; Zhang, J.X.; Murakami, R. Study on the fatigue properties of plasma nitriding S45C with a pre-ultrasonic nanocrystal surface modification process. *Surf. Coat. Technol.* **2013**, *216*, 191–198. [CrossRef]

14.　Hou, X.N.; Qin, H.F.; Gao, H.Y.; Mankoci, S.; Zhang, R.X.; Zhou, X.F.; Ren, Z.C.; Doll, G.L.; Martini, A.; Sahai, N.; et al. A systematic study of mechanical properties, corrosion behavior and biocompatibility of AZ31B Mg alloy after ultrasonic nanocrystal surface modification. *Mater. Sci. Eng. C* **2017**, *78*, 1061–1071. [CrossRef] [PubMed]

15.　Amanov, A.; Urmanov, B.; Amanov, T.; Pyun, Y.S. Strengthening of Ti-6Al-4V alloy by high temperature ultrasonic nanocrystal surface modification technique. *Mater. Lett.* **2017**, *196*, 198–201. [CrossRef]

16.　Zhang, H.; Chiang, R.; Qin, H.F.; Ren, Z.C.; Hou, X.N.; Lin, D.; Doll, G.L.; Vasudevan, V.K.; Dong, Y.L.; Ye, C. The effects of ultrasonic nanocrystal surface modification on the fatigue performance of 3D-printed Ti64. *Int. J. Fatigue* **2017**, *103*, 136–146. [CrossRef]

17.　Yasuoka, M.; Wang, P.P.; Zhang, K.Y.; Qiu, Z.Y.; Kusaka, K.; Pyoun, Y.; Murakami, R. Improvement of the fatigue strength of SUS304 austenite stainless steel using ultrasonic nanocrystal surface modification. *Surf. Coat. Technol.* **2013**, *218*, 93–98. [CrossRef]

18.　Zhang, H.W.; Hei, Z.K.; Liu, G.; Lu, J.; Lu, K. Formation of nanostructured surface layer on AISI 304 stainless steel by means of surface mechanical attrition treatment. *Acta. Mater.* **2003**, *51*, 1871–1881. [CrossRef]

19.　Ye, C.; Telang, A.; Gill, A.S.; Suslov, S.; Idell, Y.; Zweiacker, K.; Wiezorek, J.M.K.; Zhou, Z.; Qian, D.; Mannava, S.R.; et al. Gradient nanostructure and residual stresses induced by Ultrasonic Nano-crystal Surface Modification in 304 austenitic stainless steel for high strength and high ductility. *Mater. Sci. Eng. A.* **2014**, *613*, 274–288. [CrossRef]

20.　Ma, C.; Qin, H.F.; Ren, Z.C.; O'Keeffe, S.C.; Stevick, J.; Doll, G.L.; Dong, Y.L.; Winiarski, B.; Ye, C. Increasing fracture strength in bulk metallic glasses using ultrasonic nanocrystal surface modification. *J. Alloys. Compd.* **2017**, *718*, 246–253. [CrossRef]

21.　Kheradmandfard, M.; Kashani-Bozorg, S.F.; Kim, C.L.; Hanzaki, A.Z.; Pyoun, Y.S.; Kim, J.H.; Amanov, A.; Kim, D.E. Nanostructured β-type titanium alloy fabricated by ultrasonic nanocrystal surface modification. *Ultrason. Sonochem.* **2017**, *39*, 698–706. [CrossRef] [PubMed]

22.　Mandelbrot, B.B.; Passoja, D.E.; Paullay, A.J. Fract al character of fracture surface of metals. *Nature* **1984**, *308*, 721–722. [CrossRef]

23.　Ahn, D.H.; Kim, W.; Kang, M.; Park, L.J.; Lee, S.; Kim, H.S. Plastic deformation and microstructural evolution during the shock consolidation of ultrafine copper powders. *J. Mater. Sci. Eng.* **2015**, *625*, 230–244. [CrossRef]

24. Fu, P.; Zhan, K.; Jiang, C.H. Micro-structure and surface layer properties of 18CrNiMo7-6 steel after multistep shot peening. *Mater. Des.* **2013**, *51*, 309–314. [CrossRef]

25. Turan, M.E.; Aydin, F.; Sun, Y.; Cetin, M. Residual stress measurement by strain gauge and X-ray diffraction method in different shaped rails. *Eng. Fail. Anal.* **2019**, *96*, 525–529. [CrossRef]

26. Yun, Z.; Zhenkuan, S.; Qilong, W.; Tingchao, L.; Dalei, L.; Yang, L. Improving the mechanical properties of 304 stainless steel using waterjet peening. *Mater. Sci.* **2018**, *26*, 161–167.

27. Zhang, Y.; Liu, J.P.; Chen, S.Y.; Xie, X.; Liaw, P.K.; Dahmen, K.A.; Qiao, J.W.; Wang, Y.L. Serration and noise behaviors in materials. *Prog. Mater. Sci.* **2017**, *90*, 358–460. [CrossRef]

28. Wang, Y.M.; Ma, E. Strain hardening, strain rate sensitivity, and ductility of nanostructured metals. *Mater. Sci. Eng. A* **2004**, *375–377*, 46–52. [CrossRef]